Plasma Sci. Technol. **19** (2017) 035001 (8pp) doi:10.1088/2058-6272/19/3/035001

Study of the O-mode in a relativistic degenerate electron plasma

Kalsoom AZRA[1], **Muddasir ALI**[1] **and Azhar HUSSAIN**[2]

[1] School of Natural Sciences (SNS), National University of Sciences and Technology (NUST), Islamabad 44000, Pakistan
[2] Department of Physics, Quaid-i-Azam University, Islamabad 44000, Pakistan

E-mail: azrakalsoom.nust@gmail.com

Received 18 May 2016, revised 18 October 2016
Accepted for publication 19 October 2016
Published 21 February 2017

Abstract

Using the linearized relativistic Vlasov–Maxwell equations, a generalized expression for the plasma conductivity tensor is derived. The dispersion relation for the O-mode in a relativistic degenerate electron plasma is investigated by employing the Fermi–Dirac distribution function. The propagation characteristics of the O-mode (cut offs, resonances, propagation regimes, harmonic structure) are examined by using specific values of the density and the magnetic field that correspond to different relativistic dense environments. Further, it is observed that due to the relativistic effects the cut off and the resonance points are shifted to low frequency values, as a result the propagation regime is reduced. The dispersion relations for the non-relativistic and the ultra-relativistic limits are also presented.

Keywords: O-mode, degenerate plasma, white dwarf

(Some figures may appear in colour only in the online journal)

1. Introduction

The O-mode (ordinary wave) is a high frequency electromagnetic mode that propagates perpendicular to the ambient magnetic field. As $E_1 \| B_0$, so wave dynamics is not affected by the magnetic field (fluid theory) but the role of the magnetic field becomes significant when we include ($n > 1$) higher order harmonics (kinetic theory). The ordinary waves have been studied extensively for a large number of applications including electron cyclotron resonance heating in tokamaks, ionospheric heating experiments and electron cyclotron heating in the magnetically confined plasma [1–3]. In the non-degenerate (classical) magnetized plasmas the ordinary waves have been studied by using either kinetic or fluid approach [4–7]. The dispersion relation of the O-mode for the ultra-relativistic plasma was studied both for the weak and strong magnetic field limits. In the strong magnetic field limit, it was observed that the damping becomes noticeable for small values of the wave number, k, but with increase in the strength of magnetic field it is reduced. In case of the weak magnetic field, the wave characteristics remain the same as that for the non-relativistic plasma [8, 9]. The growth rate and propagation characteristics of the O-mode were investigated by Zaheer *et al* in a homogeneous relativistic plasma environment [10]. Bashir *et al* examined modification of the O-mode due to the temperature anisotropy by Vlasov approach for the non-relativistic (Maxwellian) plasma [11]. Cairns *et al* derived a relativistic theory for the damping of the O-mode and observed that due to the relativistic mass variation the resonance points spread out [12]. Pesic *et al* studied absorption and propagation characteristics of the O-mode in the relativistic plasma by numerical techniques. It was observed that at temperature $T = 200$–500 keV, the cut off density becomes two to four times as compared to the cut off density for the cold plasma [7]. Farrel *et al* presented a theory of the O-mode by using bi-Maxwellian distribution function for application to interplanetary type II. It was observed that the electrons resonate with the wave because its phase speed becomes very low in different environments like planetary magnetospheres [13].

There exist some plasma environments with high particle densities, where degenerate effects may play an important

role on the propagation characteristics of the waves [14]. In recent years, the degenerate (quantum) plasma has received much importance due to its applications in different environments, including laboratory plasmas (fusion experiments) and astrophysical plasmas (white dwarfs, neutron stars). Although it is a growing research field but only a limited literature has appeared for the O-mode in the degenerate plasma. Alexandrov *et al*, analyzed the propagation characteristics of the ordinary wave in the non-relativistic degenerate electron plasma for $\omega_p^2 \gg \omega_c^2 \gg \omega^2$ where $\omega_p = \sqrt{4\pi n_0 e^2/m_0}$ is plasma frequency and $\omega_c = eB_0/m_0 c$ is cyclotron frequency. By taking the contribution of $n = 0$ term and using limit $\frac{kv_F}{\omega_c} \gg 1$ (v_F is Fermi velocity), it was noticed that the high density plasma becomes transparent for the propagation of low frequency waves [15]. The dynamics of the ordinary wave for the relativistic dense electron plasma in a weak field limit ($\omega_p > \omega_c$) was examined by Abbas *et al*. The effect of equilibrium magnetic field is minimized due to the relativistic effects, that results in shifting of the cut offs and resonances to the lower frequency regions [16]. Recently O-mode instability in the magnetized degenerate (anisotropic) plasmas is studied by using kinetic treatment [17].

In the degenerate plasmas, the equilibrium number density of the constituent particles is much higher than in the non-degenerate plasmas. So for the degenerate plasmas, Fermi statistics is used instead of the Maxwell–Boltzmann statistics. The main ingredient of the Fermi statistics is the Fermion i.e., spin half particle. The degenerate plasmas can be found in highly dense environments like neutron stars, magnetars and white dwarfs. In the non-degenerate plasmas, average spacing between particles is large (i.e., low particle concentration) as compared to the thermal de-Broglie wavelength ($\lambda = h/\sqrt{2\pi m k_B T}$), so the wave functions will not overlap. Whereas in the degenerate plasmas, the equilibrium number density of the constituents is so large that the average inter-particle distance becomes comparable to the thermal de-Broglie wavelength. As a result the wave functions will overlap and particles will become indistinguishable. So we can say that for $n\lambda^3 > 1$ the degeneracy effects come into play [14, 18].

The present work is organized as follows: In section 2, we present the mathematical formalism for the generalized expression of the plasma conductivity tensor. In section 3, we present a generalized expression for the O-mode in the relativistic degenerate electron plasma along with some limiting cases. Finally, in section 4, we give graphical analysis of the dispersion relations and discuss some important results. In section 5, a conclusion of the manuscript is presented.

2. Mathematical formalism

After linearizing Maxwell's equations, we get

$$\omega^2\mathbf{E} - c^2k^2\mathbf{E} + c^2\mathbf{k}(\mathbf{k}\cdot\mathbf{E}) = -4\pi i\omega\mathbf{J}, \tag{1}$$

where the current density is given by

$$\mathbf{J} = \underline{\sigma}\cdot\mathbf{E},$$

or we can write it in component form

$$J_i = \sigma_{ij}E_j, \tag{2}$$

where σ_{ij} is the plasma conductivity tensor. Using equation (1)

$$[(\omega^2 - c^2k^2)\delta_{ij} + c^2k_ik_j + 4\pi i\omega\sigma_{ij}]E_j = 0,$$

where

$$R_{ij} = (\omega^2 - c^2k^2)\delta_{ij} + c^2k_ik_j + 4\pi i\omega\sigma_{ij}, \tag{3}$$

R_{ij} is a dyadic that can be written in the form of a 3×3 matrix.

$$\text{As} \quad E_j \neq 0, \quad \text{so} \quad R_{ij} = 0. \tag{4}$$

From the linearized relativistic Vlasov equation [19], given as

$$\frac{\partial f_1}{\partial t} + \mathbf{v}\cdot\frac{\partial f_1}{\partial \mathbf{x}} + e\left[\frac{\mathbf{v}\times\mathbf{B}_0}{c}\right]\cdot\frac{\partial f_1}{\partial \mathbf{p}} + e\left[\mathbf{E}_1 + \frac{\mathbf{v}\times\mathbf{B}_1}{c}\right]\cdot\frac{\partial f_0}{\partial \mathbf{p}} = 0, \tag{5}$$

we get the expression for the plasma conductivity tensor σ_{ij} (in spherical polar coordinates) [19], given by

$$\sigma_{ij} = \frac{e^2}{\omega}\int_0^\infty\int_0^\pi\int_0^{2\pi} p^2\sin\theta\,\mathrm{d}p\mathrm{d}\theta\mathrm{d}\phi\frac{v_i}{\Omega}\int_{-\infty}^{\phi}\mathrm{d}\phi' \times \exp\left[\frac{1}{\Omega}\int_{\phi'}^{\phi}(-i\omega + i\mathbf{k}\cdot\mathbf{v}'')\mathrm{d}\phi''\right] \times [(\omega - \mathbf{k}\cdot\mathbf{v}')\delta_{\beta l} + v_j'k_l]\frac{\partial f_0}{\partial p'_l}, \tag{6}$$

where $\mathbf{v}$ is the relativistic velocity, $\Omega = \omega_c/\gamma$ is the relativistic electron cyclotron frequency and the relativistic factor is given by $\gamma = \sqrt{1 + p^2/m_0^2c^2}$.

3. Generalized expression for the O-mode

In order to study the O-mode by using kinetic theory, we need zz component of the plasma conductivity tensor [19], given by

$$\sigma_{zz} = -2\pi ie^2\int_0^\infty p^2\frac{\partial f_0}{\partial p}\mathrm{d}p\int_0^\pi v\sin\theta\cos^2\theta \times \sum_{n=-\infty}^{\infty} J_n^2(\zeta\sin\theta)\frac{\mathrm{d}\theta}{(\omega - k_z v\cos\theta - n\Omega)}, \tag{7}$$

where J_n is the Bessel function and $\zeta = k_x v/\Omega$. As the O-mode is a perpendicularly propagating mode, so we

will take $k_z = 0$ in the above equation. After performing angle integration and using summation over n, we obtain

$$\sigma_{zz} = -\frac{4\pi i e^2}{3\omega}\int_0^\infty vp^2\frac{\partial f_0}{\partial p}\mathrm{d}p \times {}_1F_2\left[\left\{\frac{1}{2}\right\},\left\{\frac{5}{2},1\right\},-\left(\frac{k_x v}{\Omega}\right)^2\right] - 4\pi i e^2\int_0^\infty vp^2\frac{\partial f_0}{\partial p}\mathrm{d}p\sum_{n=1}^{\infty}\frac{\left(\frac{k_x v}{\Omega}\right)^{2n}}{(2n+3)\Gamma(2n+2)} \times {}_1F_2\left[\left\{\frac{1}{2}+n\right\},\left\{\frac{5}{2}+n,1+2n\right\},-\left(\frac{k_x v}{\Omega}\right)^2\right] \times\left\{\frac{1}{\omega-n\Omega}+\frac{1}{\omega+n\Omega}\right\}. \quad (8)$$

In order to solve the above integral, we have used

$$\int_0^\pi \sin\theta\cos^2\theta J_n^2(\zeta\sin\theta)\mathrm{d}\theta = \frac{2\zeta^{2n}}{(2n+3)\Gamma(2n+2)} \times {}_1F_2\left[\left\{\frac{1}{2}+n\right\},\left\{\frac{5}{2}+n,1+2n\right\},-\zeta^2\right], \quad (9)$$

and

$$\int_0^\pi \sin\theta\cos^2\theta J_0^2(\zeta\sin\theta)\mathrm{d}\theta = \frac{2}{3} \times {}_1F_2\left[\left\{\frac{1}{2}\right\},\left\{\frac{5}{2},1\right\},-\zeta^2\right], \quad (10)$$

where ${}_1F_2\left[\left\{\frac{1}{2}+n\right\},\left\{\frac{5}{2}+n,1+2n\right\},-\zeta^2\right]$ is the hypergeometric function.

3.1. Relativistic degenerate (quantum) case

To represent highly dense environments, the Fermi–Dirac distribution function is used.

$$f_0(E) = \left(1+\exp\left[\frac{E-E_\mathrm{F}}{k_\mathrm{B}T}\right]\right)^{-1}, \quad (11)$$

where E is the relativistic energy. The relativistic Fermi energy (E_F) [16] is given by

$$E_\mathrm{F}^2 = p_\mathrm{F}^2c^2 + m_0^2c^4,$$

where p_F is (magnitude of) the relativistic Fermi momentum. It can be easily checked that in the limit $T \to 0$, the derivative of the above distribution function takes the form of a step function, which means that all energy levels below the Fermi energy are filled and those above are vacant [15].

$$\frac{\partial f_0}{\partial E} = \frac{-2}{(2\pi\hbar)^3}\delta(E_\mathrm{F}-E), \quad (12)$$

where δ is the Dirac delta function and $\hbar$ is reduced Planck's constant. For the relativistic case, we can write equation (8) as

$$\sigma_{zz} = -\frac{4\pi i e^2}{3\omega}\int_{m_0c^2}^\infty\frac{(E^2-m_0^2c^4)^{\frac{3}{2}}}{cE}\frac{\partial f_0}{\partial E}\mathrm{d}E \times {}_1F_2\left[\left\{\frac{1}{2}\right\},\left\{\frac{5}{2},1\right\},-\frac{k_x^2(E^2-m_0^2c^4)}{e^2B_0^2}\right] - 4\pi i e^2\int_{m_0c^2}^\infty(E^2-m_0^2c^4)^{\frac{3}{2}}\frac{\partial f_0}{\partial E}\mathrm{d}E \times\sum_{n=1}^{\infty}\frac{(E^2-m_0^2c^4)^n}{cE(2n+3)\Gamma(2n+2)}\left(\frac{k_x}{eB_0}\right)^{2n} \times {}_1F_2\left[\left\{\frac{1}{2}+n\right\},\left\{\frac{5}{2}+n,1+2n\right\},-\frac{k_x^2(E^2-m_0^2c^4)}{e^2B_0^2}\right] \times\left\{\frac{1}{\omega-\frac{neB_0c}{E}}+\frac{1}{\omega+\frac{neB_0c}{E}}\right\}, \quad (13)$$

where $n_0 = p_\mathrm{F}^3/3\pi^2\hbar^3$ [14, 16, 20–23]. Using the value of σ_{zz} from equation (13) in equation (3), we get the expression for the O-mode in the relativistic degenerate plasma.

$$\omega^2 = \frac{\omega_\mathrm{p}^2}{\sqrt{1+\frac{p_\mathrm{F}^2}{m_0^2c^2}}} \times {}_1F_2\left[\left\{\frac{1}{2}\right\},\left\{\frac{5}{2},1\right\},-\frac{c^2k_x^2}{\omega_\mathrm{c}^2}\frac{p_\mathrm{F}^2}{m_0^2c^2}\right] + c^2k_x^2 + 3\omega_\mathrm{p}^2\sum_{n=1}^{\infty}\left(\frac{p_\mathrm{F}}{m_0c}\right)^{2n}\left(\frac{ck_x}{\omega_\mathrm{c}}\right)^{2n} \times\frac{1}{(2n+3)\Gamma(2n+2)} \times {}_1F_2\left[\left\{\frac{1}{2}+n\right\},\left\{\frac{5}{2}+n,1+2n\right\},-\frac{c^2k_x^2}{\omega_\mathrm{c}^2}\frac{p_\mathrm{F}^2}{m_0^2c^2}\right] \times\left\{\frac{1}{\left(\sqrt{1+\frac{p_\mathrm{F}^2}{m_0^2c^2}}-\frac{n\omega_\mathrm{c}}{\omega}\right)}+\frac{1}{\left(\sqrt{1+\frac{p_\mathrm{F}^2}{m_0^2c^2}}+\frac{n\omega_\mathrm{c}}{\omega}\right)}\right\}. \quad (14)$$

From equation (14), we can discuss two special cases i.e., the non-relativistic case and the ultra-relativistic case. The quantum relativistic effects can be defined by the parameter p_F/m_0c. For the non-relativistic case we have $p_F/m_0c \ll 1$, for the semi-relativistic case $p_F/m_0c < 1$, for the relativistic case $p_F/m_0c > 1$ and for the ultra-relativistic case $p_F/m_0c \gg 1$ [14, 22, 24].

(1) *Non-relativistic degenerate case*. For the non-relativistic degenerate electron plasma ($p_F \ll m_0c$), the dispersion relation of the O-mode takes the form

$$\omega^2 = \omega_p^2 \times {}_1F_2\left[\left\{\frac{1}{2}\right\}, \left\{\frac{5}{2}, 1\right\}, -\frac{v_F^2k_x^2}{\omega_c^2}\right] + c^2k_x^2 + 3\omega_p^2\sum_{n=1}^{\infty}\left(\frac{v_Fk_x}{\omega_c}\right)^{2n}\frac{1}{(2n+3)\Gamma(2n+2)} \times {}_1F_2\left[\left\{\frac{1}{2}+n\right\}, \left\{\frac{5}{2}+n, 1+2n\right\}, -\frac{v_F^2k_x^2}{\omega_c^2}\right] \times \left\{\frac{1}{\left(1-\frac{n\omega_c}{\omega}\right)} + \frac{1}{\left(1+\frac{n\omega_c}{\omega}\right)}\right\}, \quad (15)$$

where v_F is the Fermi velocity.

(2) *Ultra-relativistic degenerate case*. For the ultra-relativistic degenerate electron plasma ($p_F \gg m_0c$) the dispersion relation of the O-mode takes the form

$$\omega^2 = \omega_{pF}^2 \times {}_1F_2\left[\left\{\frac{1}{2}\right\}, \left\{\frac{5}{2}, 1\right\}, -\frac{c^2k_x^2}{\omega_{cF}^2}\right] + c^2k_x^2 + 3\omega_{pF}^2\sum_{n=1}^{\infty}\left(\frac{ck_x}{\omega_{cF}}\right)^{2n}\frac{1}{(2n+3)\Gamma(2n+2)} \times {}_1F_2\left[\left\{\frac{1}{2}+n\right\}, \left\{\frac{5}{2}+n, 1+2n\right\}, -\frac{c^2k_x^2}{\omega_{cF}^2}\right] \times \left\{\frac{1}{\left(1-\frac{n\omega_{cF}}{\omega}\right)} + \frac{1}{\left(1+\frac{n\omega_{cF}}{\omega}\right)}\right\}, \quad (16)$$

where $\omega_{cF} = eB_0/p_F$ and $\omega_{pF} = \sqrt{4\pi n_0e^2c/p_F}$ are the cyclotron frequency and the plasma frequency for the ultra-relativistic degenerate case [16].

4. Graphical representation and discussion

For the graphical representation of the O-mode we choose different values of the equilibrium number density and the magnetic field that correspond to various environments. One of the environments is a white dwarf where the magnetic field and the equilibrium number density may vary in different regions [14, 25]. The equilibrium number density of electrons in the outer mantle of a white dwarf is in the range 10^{26}–10^{28} cm^{-3}, so they can be treated as non-relativistic. On the surface of a white dwarf the electrons are relativistic corresponding to the equilibrium number densities in the range 10^{29}–10^{31} cm^{-3}. Similarly in the core of a white dwarf electron's equilibrium number density is in the range 10^{32}–10^{34} cm^{-3}, which is the ultra-relativistic case. The temperature of a white dwarf in the outer mantle, surface and core lies in the range 10^7–10^9 K [26].

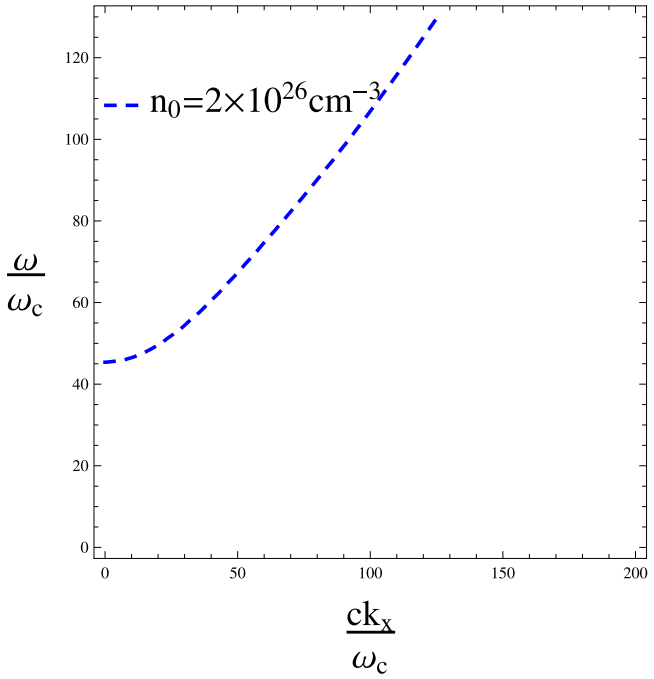

Figure 1. Plot of ω versus ck_x for the O-mode in the non-relativistic degenerate plasma with the equilibrium number density $n_0 = 2\times 10^{26}$ cm^{-3} and the equilibrium magnetic field $B_0 = 10^9$ G.

4.1. Non-relativistic degenerate case

In figure 1, a plot of the O-mode in the quantum (degenerate) case is presented (using equation (15)). For the degenerate case we use the parameters of the white dwarf environment i.e., $n_0 = 2 \times 10^{26}$ cm^{-3} and $B_0 = 10^9$ G. We can easily observe that the O-mode is propagating in the non-relativistic degenerate plasma at much higher frequency. As the degenerate plasmas are extremely dense, so the ratio of the plasma frequency to the cyclotron frequency is high i.e., $\frac{\omega_p}{\omega_c} = 45.38$. In figure 2, we have presented a plot between $\frac{\omega^2}{c^2k_x^2}$ (inverse of the square of refractive index) and $\frac{\omega}{\omega_p}$ for the non-relativistic degenerate case. The graph presented in figure 2 is similar to the ones given in the text books for non-relativistic case [2]. To observe the harmonics of the electron cyclotron

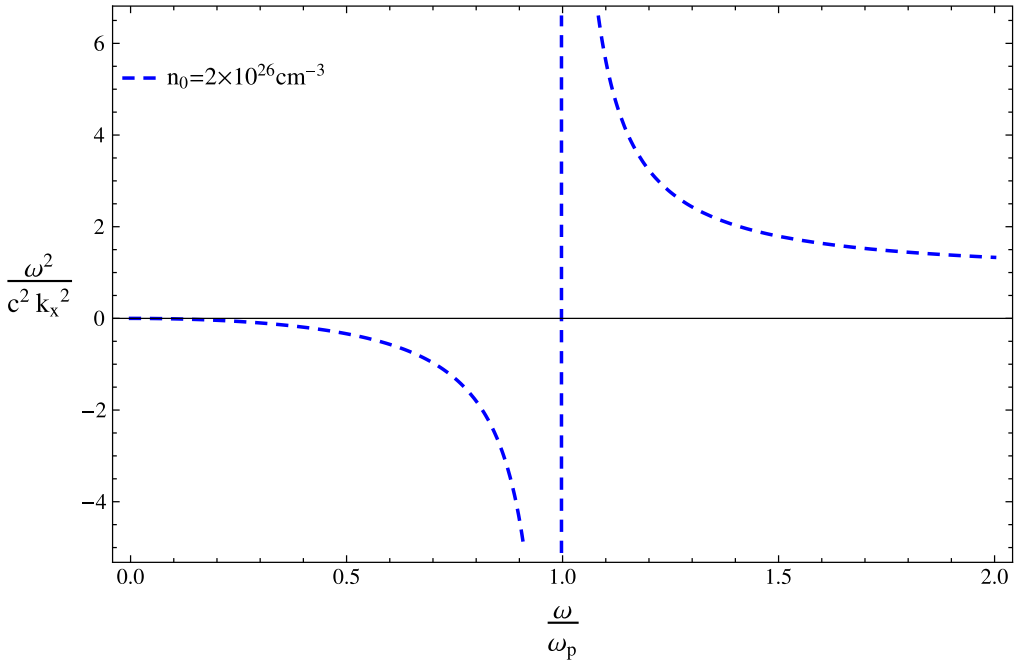

Figure 2. Plot between inverse of the square of refractive index $\left(\frac{\omega^2}{c^2k_x^2} = \frac{1}{\tilde{n}^2}\right)$ and $\frac{\omega}{\omega_p}$ for the O-mode in the non-relativistic degenerate plasma with the equilibrium number density $n_0 = 2 \times 10^{26}$ cm^{-3} and the equilibrium magnetic field $B_0 = 10^9$ G.

frequency in the non-relativistic degenerate plasma we use equation (15). If we reduce the propagation regime in figure 1 and focus on the lower values of the normalized frequency $\left(\frac{\omega}{\omega_c}\right)$ we will get the cyclotron harmonic resonance structure which is shown in figure 3. The dispersion curves in figure 3 are obtained by keeping summation on n ($n = 1$–3) in equation (15). The dispersion curves show that the wave is propagating exactly at the harmonics of the electron cyclotron frequency.

Ichimaru *et al* analyzed the behavior of the O-mode in a non-relativistic non-degenerate plasma for $\omega_p \ll \omega_c$ and $\omega_c \ll \omega_p$. The dispersion curves in our case are in excellent agreement with the curves given by Ichimaru for the low values of density [27]. At higher densities the curves become oscillatory for large values of k.

4.2. Relativistic degenerate case

There are several references available for the relativistic non-degenerate case. Some authors have studied the propagation characteristics of the O-mode for the relativistic Maxwellian plasma in different electron temperature ranges by using numerical techniques [7]. Zaheer *et al* derived the dispersion relation of the O-mode for a strongly magnetized case by using the asymptotic value of the Bessel function

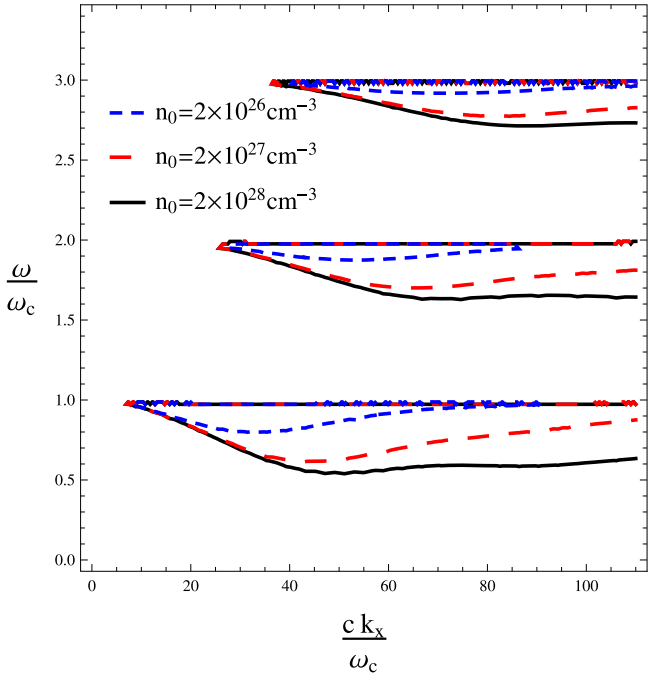

Figure 3. The dispersion characteristics of the O-mode around the first three harmonics of the electron cyclotron frequency in the non-relativistic degenerate plasma. Each dispersion curve corresponds to a different value of equilibrium number density for the first three harmonics. The equilibrium magnetic field is constant i.e., $B_0 = 10^9$ G.

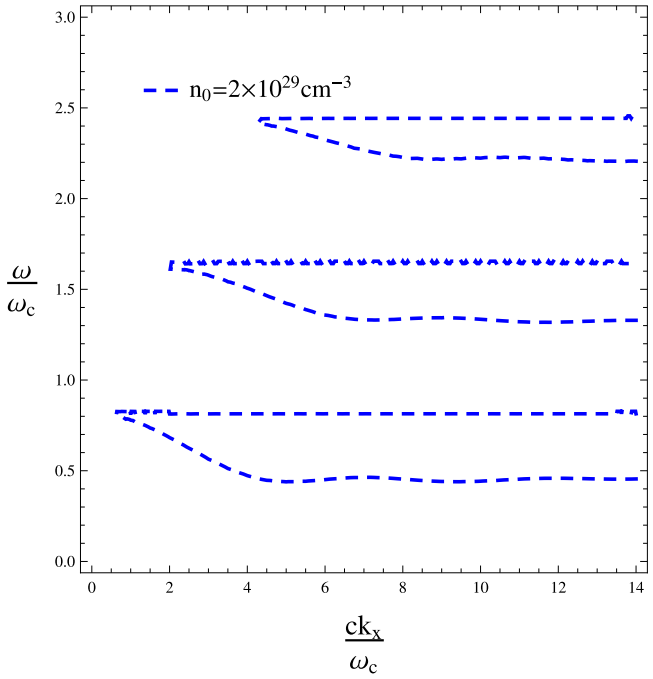

Figure 4. The dispersion characteristics of the O-mode around the first three harmonics of the (electron) cyclotron frequency in the weakly relativistic degenerate plasma with $n_0 = 2 \times 10^{29}$ cm^{-3} and $B_0 = 10^{10}$ G.

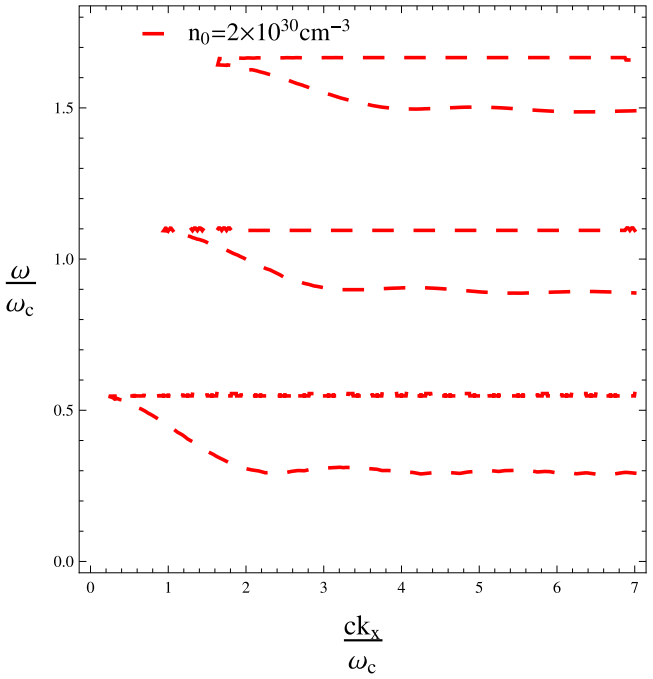

Figure 5. The dispersion characteristics of the O-mode around the first three harmonics of the (electron) cyclotron frequency in the relativistic degenerate plasma with $n_0 = 2 \times 10^{30}$ cm^{-3} and $B_0 = 10^{10}$ G.

[10]. Abbas *et al* analyzed the O-mode for a weakly magnetized case [9].

In a degenerate plasma the equilibrium number density will decide whether we are in a weakly relativistic (10^{29} cm^{-3}), relativistic (10^{30} cm^{-3}) or strongly relativistic (10^{31} cm^{-3}) regime. In the relativistic degenerate case the Fermi momentum is greater than the rest mass momentum (i.e., $p_F > m_0 c$), so we have to choose the density in the range 10^{29}–10^{31} cm^{-3}. We can find such densities in the white dwarf environment where the magnetic field is of the order of 10^{10} G. The graphs presented in figures 4–6 show that the dispersion curves do not occur at the exact harmonics of the electron cyclotron frequency instead they are shifted downward due to the Lorentz factor. In figure 7, we present a plot between $\frac{\omega^2}{c^2 k_x^2}$ and $\frac{\omega}{\omega_p}$ for the weakly relativistic (2×10^{29} cm^{-3}), relativistic (2×10^{30} cm^{-3}) and strongly relativistic (2×10^{31} cm^{-3}) degenerate plasma. In the non-relativistic degenerate case shown in figure 2, it can be seen that the cut off occurs exactly at $\omega = \omega_p$ whereas in figure 7 (relativistic degenerate case) the cut off occurs at $\omega < \omega_p$ due to the relativistic variation of the mass. As the equilibrium number density increases, the cut offs shift to the lower values of frequency as expected. We have used $\frac{ck_x}{\omega_c} = 4.5, 2.2, 0.9$ for the weakly relativistic, relativistic and strongly relativistic cases, respectively.

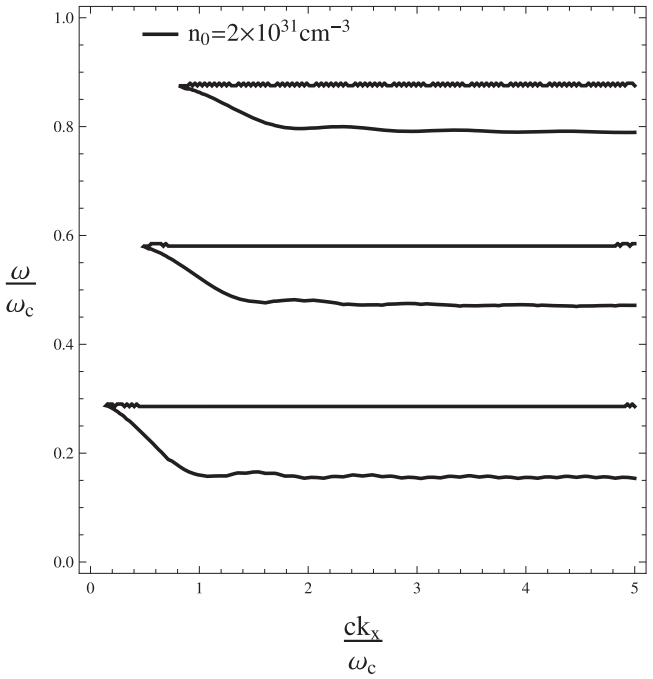

Figure 6. The dispersion characteristics of the O-mode around the first three harmonics of the (electron) cyclotron frequency in the strongly relativistic degenerate plasma with $n_0 = 2 \times 10^{31}$ cm^{-3} and $B_0 = 10^{10}$ G.

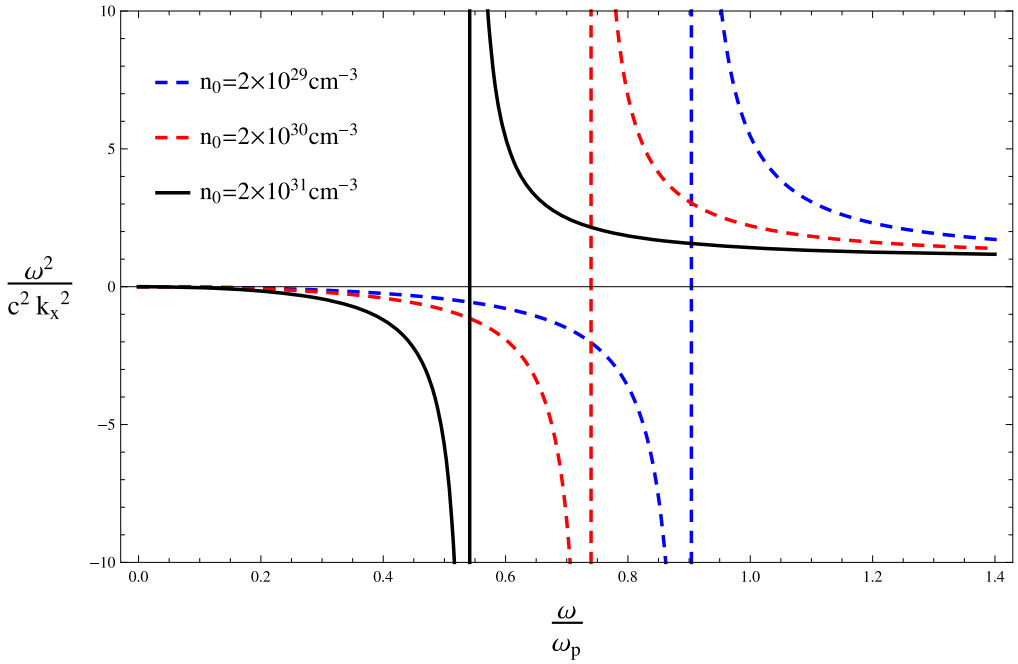

Figure 7. Plot between inverse of the square of refractive index $\left(\frac{\omega^2}{c^2k_x^2} = \frac{1}{\tilde{n}^2}\right)$ and $\frac{\omega}{\omega_p}$ for the O-mode in the weakly relativistic, relativistic and strongly relativistic degenerate plasma with the equilibrium number density $n_0 = 2 \times 10^{29}$–2×10^{31} cm^{-3} and the equilibrium magnetic field $B_0 = 10^{10}$ G.

4.3. Ultra-relativistic degenerate case

In the ultra-relativistic degenerate case ($p_F \gg m_0c$), the corresponding equilibrium number densities lie in the range 10^{32}–10^{34} cm^{-3} and the value of the equilibrium magnetic field that we have chosen is 10^{12} G. The dispersion relation of the O-mode in the ultra-relativistic degenerate plasma is given by the equation (16). To plot this dispersion relation we have normalized ω and ck_x by ω_{cF} and we are taking ω_{pF}/ω_{cF} instead of ω_p/ω_c. In figure 8, we have presented the harmonic structure of the O-mode in the ultra-relativistic degenerate plasma. The cyclotron harmonics become more oscillatory in the ultra-relativistic case as compared to the non relativistic case as shown in figure 8. The graph presented for the ultra-relativistic degenerate case (figure 9) is exactly the same as that of figure 2 but here we have normalized it with a different parameter. The O-mode is propagating for $\omega > \omega_{pF}$; at $\omega = \omega_{pF}$ there is a cut off and beyond the cut off point i.e., $\omega < \omega_{pF}$ there is a non-propagation region.

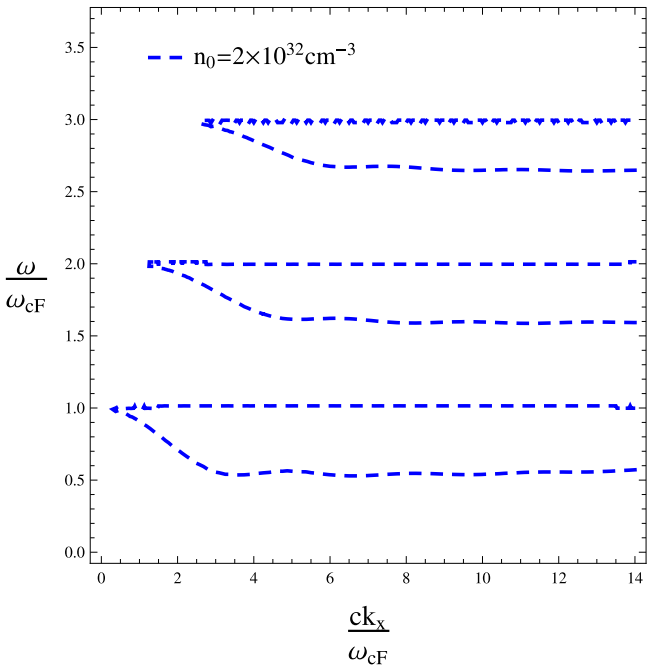

Figure 8. The dispersion characteristics of the O-mode around the first three harmonics of the (electron) cyclotron frequency in the ultra-relativistic degenerate plasma with $n_0 = 2 \times 10^{32}$ cm^{-3} and $B_0 = 10^{12}$ G.

5. Conclusion

Using the linearized relativistic Vlasov–Maxwell equations, the dispersion relation of the O-mode in a relativistic degenerate electron plasma is derived along with two limiting cases. The results are analyzed and discussed for non-relativistic,

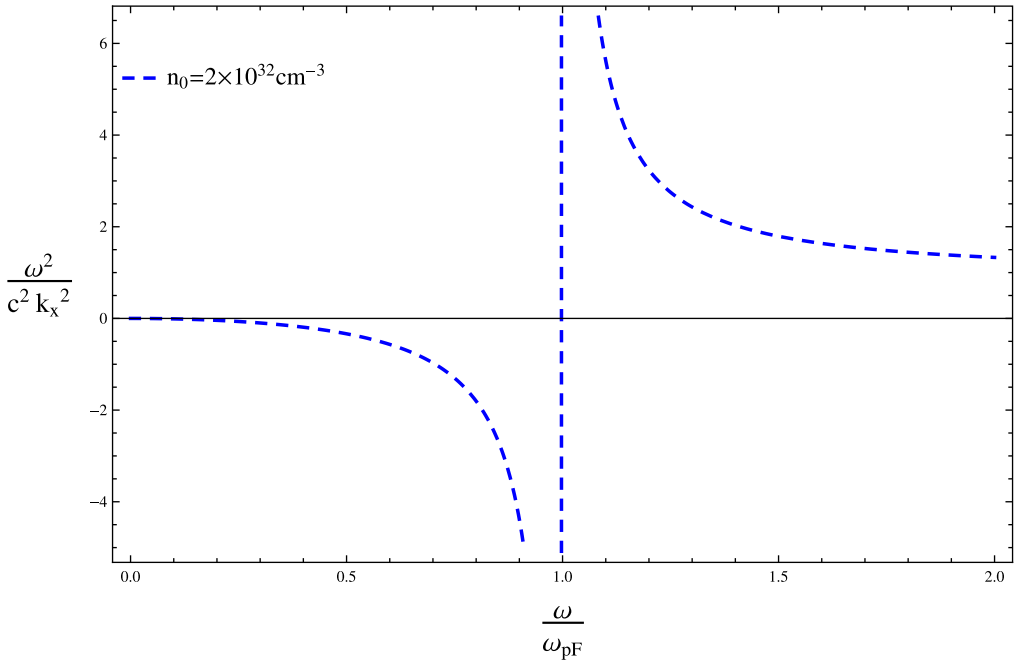

Figure 9. Plot between inverse of the square of refractive index $\left(\frac{\omega^2}{c^2k_x^2} = \frac{1}{\hat{n}^2}\right)$ and $\frac{\omega}{\omega_{pF}}$ for the O-mode in the ultra-relativistic degenerate plasma with the equilibrium number density $n_0 = 2 \times 10^{32}$ cm^{-3} and the equilibrium magnetic field $B_0 = 10^{12}$ G.

relativistic (weakly relativistic, relativistic, strongly relativistic) and ultra-relativistic electron plasma, whereas the ambient magnetic field ranges from 10^9-10^{12} G. It is observed that unlike non-relativistic degenerate case, the dispersion curves are shifted downward due to the Lorentz factor in the relativistic degenerate case. Further, as we move from weakly relativistic to strongly relativistic regions, a shift in cut-off and resonance points to lower frequency values is observed due to the relativistic effects.

References

[1] Guest G 2009 *Electron Cyclotron Heating of Plasmas* (Weinheim: Wiley-VCH Verlag GmbH and Co. KGaA)
[2] Chen F F 1984 *Introduction to Plasma Physics and Controlled Fusion* (New York: Plenum)
[3] Cheo B R and Kuo S P 1981 *Phys. Fluids* **24** 784
[4] Nambu M 1974 *Phys. Fluids* **17** 1885
[5] Sodha M S *et al* 1980 *Proc. Indian Nat. Sci. Acad.* **46** 343
[6] McDonald D C *et al* 1998 *Phys. Plasmas* **5** 883
[7] Nikolic L J and Pesic S 1998 *Plasma Phys. Control. Fusion* **40** 1373
[8] Ali M, Zaheer S and Murtaza G 2010 *Prog. Theor. Phys.* **124** 1083
[9] Abbas G, Murtaza G and Kingham R J 2010 *Phys. Plasmas* **17** 072105
[10] Zaheer S and Murtaza G 2008 *Phys. Scr.* **77** 035503
[11] Bashir M F and Murtaza G 2012 *Braz. J. Phys.* **42** 487
[12] Cairns R A and LashmoreDavies C N 1982 *Phys. Fluids* **25** 1605
[13] Farrell W M 2011 *J. Geophys. Res.* **106** 15701-15709
[14] Khan S A 2012 *Phys. Plasmas* **19** 014506
[15] Alexandrov A F, Bogdankevich L S and Rukhadze A A 1984 *Principles of Plasma Electrodynamics* (Berlin: Springer)
[16] Abbas G, Bashir M F and Murtaza G 2012 *Phys. Plasmas* **19** 072121
[17] Iqbal Z *et al* 2014 *Phys. Plasmas* **21** 032128
[18] Roy B N 2002 *Fundamentals of Classical and Statistical Thermodynamics* (New York: Wiley)
[19] Montgomery D C and Tidman D A 1964 *Plasma Kinetic Theory* (New York: McGraw-Hill)
[20] Pathria R K and Beale P D 2011 *Statistical Mechanics* (Oxford: Academic)
[21] Huang K 1963 *Statistical Mechanics* (New York: Wiley)
[22] Chandra S, Maji P and Ghosh B 2014 *Int. J. Math. Comput. Phys. Electr. Comput. Eng.* **8** 5
[23] Akbari-Moghanjoughi M 2011 *Phys. Plasmas* **18** 012701
[24] Akbari-Moghanjoughi M and Kalejahi A E 2013 *J. Plasma Phys.* **79** 1081
[25] Shah H A *et al* 2011 *Phys. Plasmas* **18** 102306
[26] Mahmood S, Sadiq S and Haque Q 2013 *Phys. Plasmas* **20** 122305
[27] Ichimaru S 1973 *Basic Principles of Plasma Physics: A Statistical Approach* (New York: Addison-Wesley)